

# Thermodynamic optimisation and analysis of four Kalina cycle layouts for high temperature applications

**Modi, Anish; Haglind, Fredrik**

*Published in:*
Applied Thermal Engineering

*Link to article, DOI:*
10.1016/j.applthermaleng.2014.11.047

*Publication date:*
2015

# Thermodynamic optimisation and analysis of four Kalina cycle layouts for high temperature applications

Anish Modi*, Fredrik Haglind

*Department of Mechanical Engineering, Technical University of Denmark, Nils Koppels Allé, Building 403, DK-2800 Kgs. Lyngby, Denmark*

**Abstract**

The Kalina cycle has seen increased interest in the last few years as an efficient alternative to the conventional steam Rankine cycle. However, the available literature gives little information on the algorithms to solve or optimise this inherently complex cycle. This paper presents a detailed approach to solve and optimise a Kalina cycle for high temperature (a turbine inlet temperature of 500 °C) and high pressure (over 100 bar) applications using a computationally efficient solution algorithm. A central receiver solar thermal power plant with direct steam generation was considered as a case study. Four different layouts for the Kalina cycle based on the number and/or placement of the recuperators in the cycle were optimised and compared based on performance parameters such as the cycle efficiency and the cooling water requirement. The cycles were modelled in steady state and optimised with the maximisation of the cycle efficiency as the objective function. It is observed that the different cycle layouts result in different regions for the optimal value of the turbine inlet ammonia mass fraction. Out of the four compared layouts, the most complex layout KC1234 gives the highest efficiency. The cooling water requirement is closely related to the cycle efficiency, i.e., the better the efficiency, the lower is the cooling water requirement.

*Keywords:* Kalina cycle, optimisation, genetic algorithm, solar thermal power plant

## 1. Introduction

*Corresponding author. Tel.: +45 45251910
*Email address:* anmod@mek.dtu.dk (Anish Modi)

**Nomenclature**

*Abbreviations*

| | |
|---|---|
| GA | Genetic algorithm |
| LMTD | Log mean temperature difference, °C |
| PPTD | Pinch point temperature difference, °C |

*Symbols*

| | |
|---|---|
| $\Delta T$ | temperature difference, °C |
| $\dot{m}$ | mass flow rate, kg/s |
| $\dot{Q}$ | heat rate, MW |
| $\dot{W}$ | work rate, MW |
| $\eta$ | respective component efficiency |
| $h$ | specific enthalpy, kJ/kg |
| $p$ | pressure, bar |
| $T$ | temperature, °C or K |
| $X$ | vapour quality |
| $x$ | ammonia mass fraction |
| $y$ | objective function |

*Subscripts, including components*

| | |
|---|---|
| cd1 | Condenser-1 |
| cd2 | Condenser-2 |
| gen | Generator |
| mx1 | Mixer-1 |
| mx2 | Mixer-2 |
| net | Net electrical output from the power cycle |
| pp | Pinch point temperature difference, °C |
| pp,cd | Minimum pinch point temperature difference in the condensers, °C |
| pp,re | Minimum pinch point temperature difference in the recuperators, °C |
| pu1 | Pump-1 |
| pu2 | Pump-2 |
| re1 | Recuperator-1 |
| re2 | Recuperator-2 |
| re3 | Recuperator-3 |
| re4 | Recuperator-4 |
| rec | Receiver/boiler |
| sep | Separator |
| spl | Splitter |
| thv | Throttle valve |
| tur | Turbine |

The Kalina cycle was introduced in 1984 [1] as an alternative to the conventional Rankine cycle to be used as a bottoming cycle for combined cycle power plants. It uses a mixture of ammonia and water as its working fluid, instead of pure water as in the case of a steam Rankine cycle. The composition of the ammonia-water mixture could be varied by changing the *ammonia mass fraction* which is defined as the ratio of the mass of ammonia in the mixture to the total mass of the mixture. Since its introduction, several uses for the Kalina cycle have been proposed such as in a geothermal power plant, for waste heat recovery, in solar power plants, etc. Most of the documented studies however focus on low or moderate temperature heat to power conversion applications. Ogriseck [2] presented the possibility of integration of a Kalina cycle in a combined heat and power plant. The net efficiency of the plant was calculated for different cooling water temperatures and ammonia mass fractions for the basic solution. Bombarda et al. [3] presented a thermodynamic comparison between the Kalina cycle and an organic Rankine cycle for heat recovery from diesel engines. They concluded that although the obtained electrical power outputs are nearly equal, the Kalina cycle requires a much higher turbine inlet pressure to attain the similar output, thereby making it unjustified for such use. Singh and Kaushik [4] presented energy and exergy analyses and optimisation of a Kalina cycle coupled with a coal-fired steam power plant for exhaust heat recovery. They found out that at a turbine inlet pressure of 40 bar, an ammonia mass fraction of 0.8 gives the maximum cycle efficiency. Coskun et al. [5] presented a comparison between different power cycles for a medium temperature geothermal resource. They found that the Kalina cycle and the double flash cycle provided the least levelized cost of electricity and hence the shortest payback periods. Wang et al. [6] presented a parametric analysis and optimisation of a Kalina cycle driven by solar energy. They found that the net power output and the system efficiency are less sensitive to the turbine inlet temperature under given conditions and that there exists an optimal turbine inlet pressure which results in maximum net power output. Sun et al. [7] presented an energy-exergy analysis and parameter design optimisation for a Kalina cycle with an auxiliary superheater for a low grade thermal energy conversion system using solar energy as heat input. Larsen et al. [8] presented the optimisation and a simplified cost analysis of the Kalina split-cycle using

genetic algorithm (GA) in MATLAB with primary focus on the boiler, the turbine and the mixing system subsections of the cycle. They also compared the performance of the Kalina split-cycle to that of a normal Kalina cycle. Nguyen et al. [9] conducted an exergy analysis of the Kalina split-cycle. The two studies [8,9] concluded that the Kalina split-cycle with reheat was thermodynamically better than the normal Kalina cycle but this improvement came at the price of increased initial cost and a more complex cycle design.

With regards to high temperature Kalina cycles, few studies have been made. All of these studies however suggest potential thermodynamic benefits of using the Kalina cycle, thus motivating further research in the high temperature Kalina cycle applications. The Kalina cycle layouts for high temperature applications are inherently more complex than the layouts typically used for the low temperature applications. Marston [10] presented the parametric analysis of a Kalina cycle to serve a bottoming cycle for a gas turbine power plant. Marston and Hyre [11] compared the performance of a triple-pressure steam cycle and a Kalina cycle as a gas turbine bottoming cycle. They concluded that the Kalina cycle was more efficient. Ibrahim and Kovach [12] studied the effect of varying the ammonia mass fraction and the separator temperature on the cycle efficiency for a Kalina bottoming cycle using gas turbine exhaust as the heat source. The authors found that the Kalina cycle is 10-20 % more efficient than the Rankine cycle with the same boundary conditions. Nag and Gupta [13] performed an exergy analysis of a Kalina cycle with gas turbine exhaust as the heat source. They concluded that the important parameters affecting the cycle efficiency are the turbine inlet temperature, composition and the separator temperature. Thorin [14] presented the analysis of a Kalina cycle to be used for industrial waste heat recovery, biomass based cogeneration and gas engine waste heat recovery. Various methods for calculating the thermophysical properties of the ammonia-water mixture were also presented. Modi and Haglind [15] presented the exergy analysis of a Kalina cycle for a central receiver solar thermal power plant with direct steam generation. Their results suggested the cycle layout and the number of recuperators might have an affect on the optimal conditions for the maximum cycle efficiency, and that the Kalina cycle might be beneficial if more storage based operation takes place.

None of the studies for high temperature Kalina cycles presented a detailed algorithm for solving or optimising the Kalina cycle. Marston [10] briefly presented a simplified topology of the cycle for the calculation of the mass flow rates in the cycle. For the low temperature applications, Singh and Kaushik [4] and Sun [7] presented algorithms to solve a Kalina cycle for use as a bottoming cycle and as a solar based power cycle respectively. Along with the presentation of little information on the cycle solution methodology, there were few inappropriate assumptions made in the above studies. For instance, Marston [10] assumed the pinch point in the condensers to always occur at the working fluid outlet and both Singh and Kaushik [4] and Sun [7] used an overall log mean temperature difference (LMTD) for various heat exchangers, including the evaporator and the condenser, as an input to the cycle calculation. These issues are further discussed in the Section 4 of this paper.

The primary objective of this paper is therefore to present the detailed methodology of solving and optimising a Kalina cycle for high temperature and pressure applications which serves well on both the accuracy and the computational efficiency fronts. The study also improves on the assumptions made in the previous publications such as the location and values of the pinch point temperature differences (PPTDs) while using an approach where fewer iterations were required, thus saving computational time. As a case, a central receiver solar thermal power plant operating with direct steam generation is considered. The term *direct steam generation* is used here for the ammonia-water mixtures too. In a previous study by Modi and Haglind [15], the analysis suggested that the position and the number of recuperators might affect the performance of the cycle, therefore four Kalina cycle layouts with different number and/or placement of recuperators are analysed in this paper. The presented layouts are compared with respect to the performance parameters such as the cycle efficiency and the cooling water requirement.

The paper is structured as follows: Section 2 presents the different Kalina cycle layouts and the methodology for solving and optimising the Kalina cycle, Section 3 presents the results from the optimisation of the Kalina cycle, Section 4 discusses the results and compares them with previous studies and Section 5 concludes the paper.

## 2. Methodology

The four Kalina cycle layouts compared in this paper are presented in Fig. 1. The different cycle layouts were named according to the positions of the various recuperators in the cycle. The Kalina cycle with two recuperators, termed as 'KC12', is presented in Fig. 1a, while Figs. 1b and 1c present the two layouts with three recuperators each, but at different positions and are termed as 'KC123' and 'KC234' respectively. The layout with four recuperators in the cycle, termed as 'KC1234', is presented in Fig. 1d. The cycle components in the different layouts are represented in abbreviated forms where REC is the receiver/boiler, TUR is the turbine, GEN is the generator, SEP is the vapour-liquid separator, RE$*$ is the recuperator, PU$*$ is the pump, CD$*$ is the condenser, MX$*$ is the mixer (where '$*$' denotes the respective component number), SPL is the splitter and THV is the throttling valve. The layout KC234 has been studied as a standard high temperature layout by Marston [10] and Nag and Gupta [13], whereas the layout KC12 was used in a preliminary analysis by Modi and Haglind [15]. The remaining two layouts were derived by adjusting the number and placement of the recuperators in the KC12 and the KC234 layouts.

Except for the number and the position of the recuperators, the different Kalina cycles work broadly in a similar manner. The superheated ammonia-water mixture, i.e., the working fluid solution, expands in the turbine and goes through the mixer-1 where it gets mixed with the ammonia lean liquid from the separator to reduce the ammonia mass fraction in the condenser-1. The mixed fluid after the mixer-1 is termed as the basic solution. The ammonia rich vapour from the separator is later mixed in the mixer-2 with a part of the basic solution coming from the splitter to again from the working fluid. This working fluid then goes through the condenser-2 and then the pump-2 to attain the pressure required at the turbine inlet. The external heat input to the working fluid comes in the boiler. In the case considered in this study, the boiler is a solar receiver.

The thermodynamic optimisation of the Kalina cycles was done with the maximisation of the cycle efficiency (i.e. the ratio of the net electrical power output to the heat input in

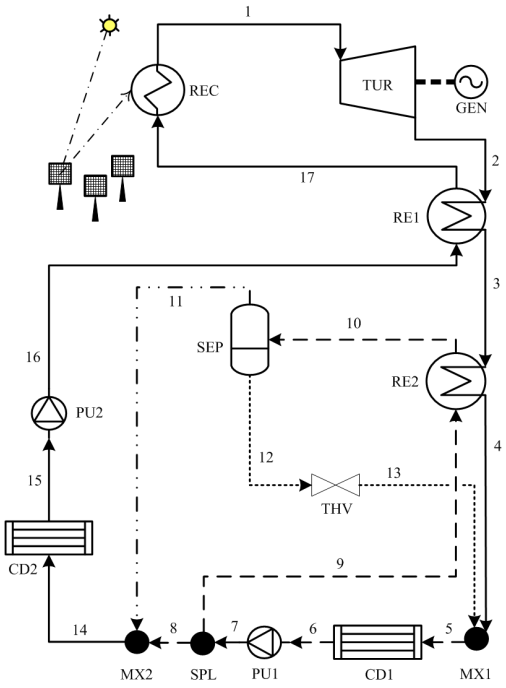


(a) Kalina cycle KC12

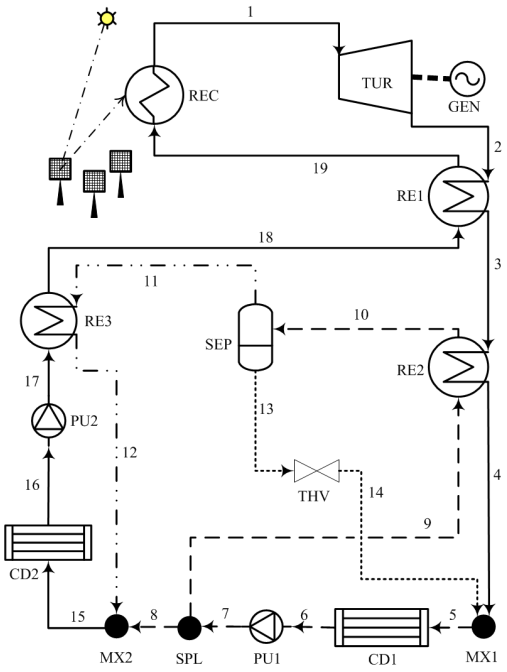


(b) Kalina cycle KC123

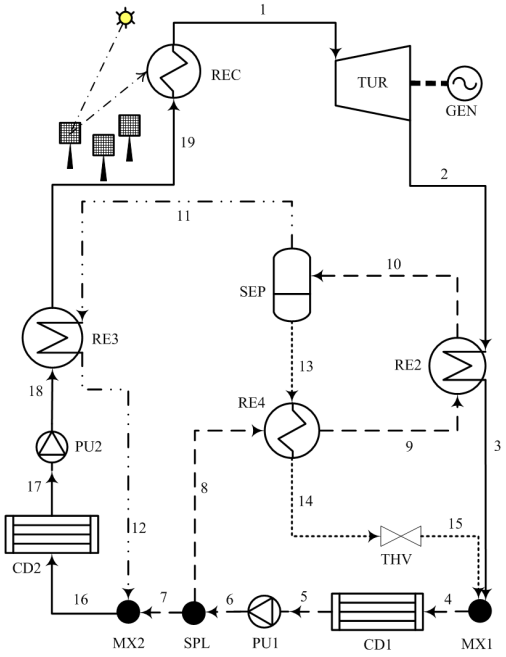


(c) Kalina cycle KC234

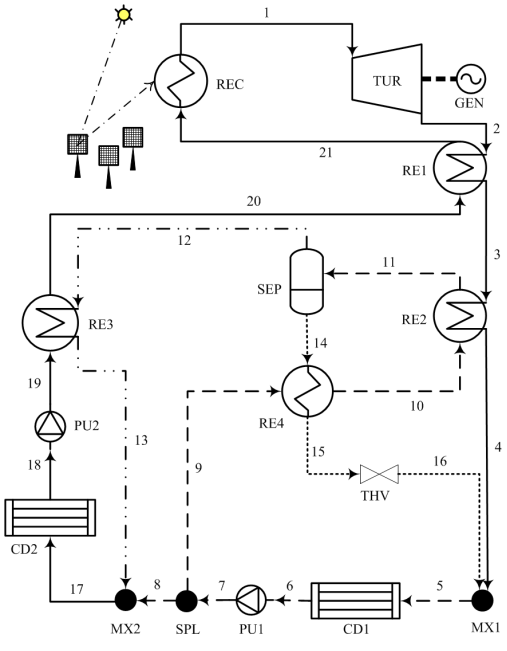


(d) Kalina cycle KC1234

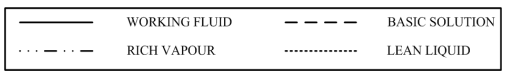


Figure 1: Various Kalina cycle layouts for high temperature applications.

the receiver) as the objective function:

$$y = \max\left(\frac{\dot{W}_{net}}{\dot{Q}_{rec}}\right) \tag{1}$$

Zhang et al. [16] highlighted that the most important parameters in the Kalina cycle performance evaluation are the ammonia mass fraction, pressure and temperature at the turbine inlet, the cycle low pressure (at turbine outlet) and the separator inlet temperature. Therefore in this study, the turbine outlet pressure, the separator inlet temperature and the separator inlet ammonia mass fraction were the decision variables while the pressure and the ammonia mass fraction at the turbine inlet were varied for parametric analysis.

The Kalina cycles were modelled in MATLAB (v2013b) [17]. The thermodynamic properties for the ammonia-water mixtures were calculated using the REFPROP (v9.1) interface for MATLAB [18]. The default property calculation method for the ammonia-water mixtures in REFPROP is using the Tillner-Roth and Friend formulation [19]. However, this formulation is highly unstable and fails to converge on several occasions, especially in the two-phase regions, near critical point and at higher ammonia mass fractions. Therefore, an alternative formulation called 'Ammonia (Lemmon)' [20] was tested and used. It was found to be more stable and with few convergence issues, without significantly compromising on the accuracy of the calculations. The specific enthalpy and the specific entropy values for about 2400 combinations of pressures, temperatures and ammonia mass fractions between 1 and 160 bar, 52 and 527 °C and 0.3 and 0.9 respectively, were compared for the two methods. The maximum and the average deviations of the Ammonia (Lemmon) formulation from the Tillner-Roth and Friend formulation for the specific enthalpy values were found to be 6.97 % and 1 %, while for the specific entropy values were found to be 4.49 % and 0.65 % respectively.

The Kalina cycle was optimised using the GA from the Optimisation Toolbox of MATLAB. The optimisation steps were as follows:

(a). The design parameters were provided as input to the GA. These included the temperature, pressure and ammonia mass fraction at the turbine inlet, the generator power

output, the efficiencies of the turbine, pumps and generator, the cooling water inlet and outlet temperatures and the minimum values of the PPTDs for the condensers and the recuperators. The lower and upper bounds for the decision variables were also provided as input.

(b). The GA then selected an initial population covering the entire search space and began the optimisation process, moving gradually towards the optimum solution with each iteration.

(c). The optimisation was performed in two steps: first with a wider range of the bounds to find out the region where the global maximum lies, then with a range close to the optimum solution. This was done to make sure that a global maximum is achieved and not a local maximum.

(d). In case there was an error in the calculation of the thermodynamic properties by REFPROP, or the mass or energy balances were not satisfied with a residual below or equal to 0.001 %, the solution was rejected.

(e). As a result of the optimisation, the cycle efficiency and the thermodynamic states at various points in the cycle were obtained.

(f). The initial population for the GA was 50, the maximum number of generations was 30, the elite count was 2, the crossover fraction was 0.8 and the function tolerance was $10^{-6}$.

In general, the following steps were used to solve the different Kalina cycles for each iteration of the optimisation process. The turbine was solved first to obtain the state at the turbine outlet. Assuming a condenser pressure for condenser-2, the mass flow rates were then obtained using a simplified configuration as presented by Marston [10]. With respect to the mass flow rates at different points in the cycle, the entire cycle can be represented by the simplified layout as shown in Fig. 2.

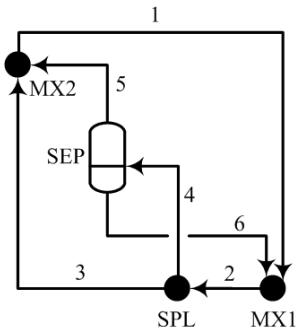


Figure 2: Simplified configuration of all the Kalina cycles with respect to different mass flow rates in the cycle.

The mass balance equations for the ammonia-water mixture and ammonia in the mixture, and the ammonia mass fraction balance equations would be:

$$\dot{m}_2 = \dot{m}_1 + \dot{m}_6 \tag{2a}$$

$$\dot{m}_2 \cdot x_2 = \dot{m}_1 \cdot x_1 + \dot{m}_6 \cdot x_6 \tag{2b}$$

$$\dot{m}_1 = \dot{m}_3 + \dot{m}_5 \tag{2c}$$

$$\dot{m}_1 \cdot x_1 = \dot{m}_3 \cdot x_3 + \dot{m}_5 \cdot x_5 \tag{2d}$$

$$\dot{m}_4 = \dot{m}_5 + \dot{m}_6 \tag{2e}$$

$$\dot{m}_4 \cdot x_4 = \dot{m}_5 \cdot x_5 + \dot{m}_6 \cdot x_6 \tag{2f}$$

$$x_2 = x_4 \tag{2g}$$

$$x_3 = x_4 \tag{2h}$$

Here, $\dot{m}$ is the mass flow rate in kg/s and $x$ is the ammonia mass fraction. The numbers 1 to 6 should be replaced by the respective stream numbers from the different layouts as shown in Table 1.

Table 1: Respective stream numbers for the different Kalina cycle layouts for simplified mass balances.

| Number in Fig. 2 | KC12 | KC123 | KC234 | KC1234 |
|---|---|---|---|---|
| 1 | 1 | 1 | 1 | 1 |
| 2 | 5 | 5 | 4 | 5 |
| 3 | 8 | 8 | 7 | 8 |
| 4 | 10 | 10 | 10 | 11 |
| 5 | 11 | 11 | 11 | 12 |
| 6 | 12 | 13 | 13 | 14 |

The mass balances presented in Eq. 2 are over the mixer-1 (Eqs. 2a and 2b), the mixer-2 (Eqs. 2c and 2d) and the separator (Eqs. 2e and 2f). The ammonia mass fraction balances are over the splitter (Eqs. 2g and 2h). On rearranging the above equations and calculating the values of the ammonia mass fractions for the two outlet streams of the separator using the state at the separator inlet as input, the following relations were obtained:

$$\frac{\dot{m}_4}{\dot{m}_1} = \frac{x_1 - x_4}{X_4 \cdot (x_5 - x_4)} \tag{3a}$$

$$\frac{\dot{m}_3}{\dot{m}_1} = \frac{x_5 - x_1}{x_5 - x_4} \tag{3b}$$

Here, $\dot{m}$ is the mass flow rate in kg/s, $x$ is the ammonia mass fraction and $X$ is the vapour quality. These relations were then used to calculate the different mass flow rates after assuming $\dot{m}_1$ to be 1 kg/s as an initial guess value. This was done repeatedly until the PPTD in the condenser-2 became greater than or equal to the minimum PPTD value for the condensers. Once the mass flow rates at different points in the cycle became known and it was made sure that the inlet stream to the separator is in two-phase flow, then the pumps, mixers, recuperators and the condensers were solved while satisfying all the design constraints such as minimum PPTD, minimum vapour quality at the turbine outlet, etc. (see assumptions below). The cycle efficiency from each iteration (with different values of the decision variables) was compared and the solution with the highest cycle efficiency was stored as the optimal solution for the given input of the turbine inlet pressure and ammonia

mass fraction. The same procedure was then repeated for different values of the turbine inlet pressures and ammonia mass fractions to evaluate the trend in the cycle performance. As an example, the detailed solution algorithm for the layout KC1234 is presented in Fig. 3. The other layouts were solved in a similar manner. It may be observed from Fig. 3 that instead of using an overall LMTD value, a more general pinch point approach was used to make sure that there were no second law violations in the heat exchangers. All the heat exchangers, including the condensers, were divided into 50 control volumes and solved so that the position of the PPTD could be calculated with sufficient accuracy.

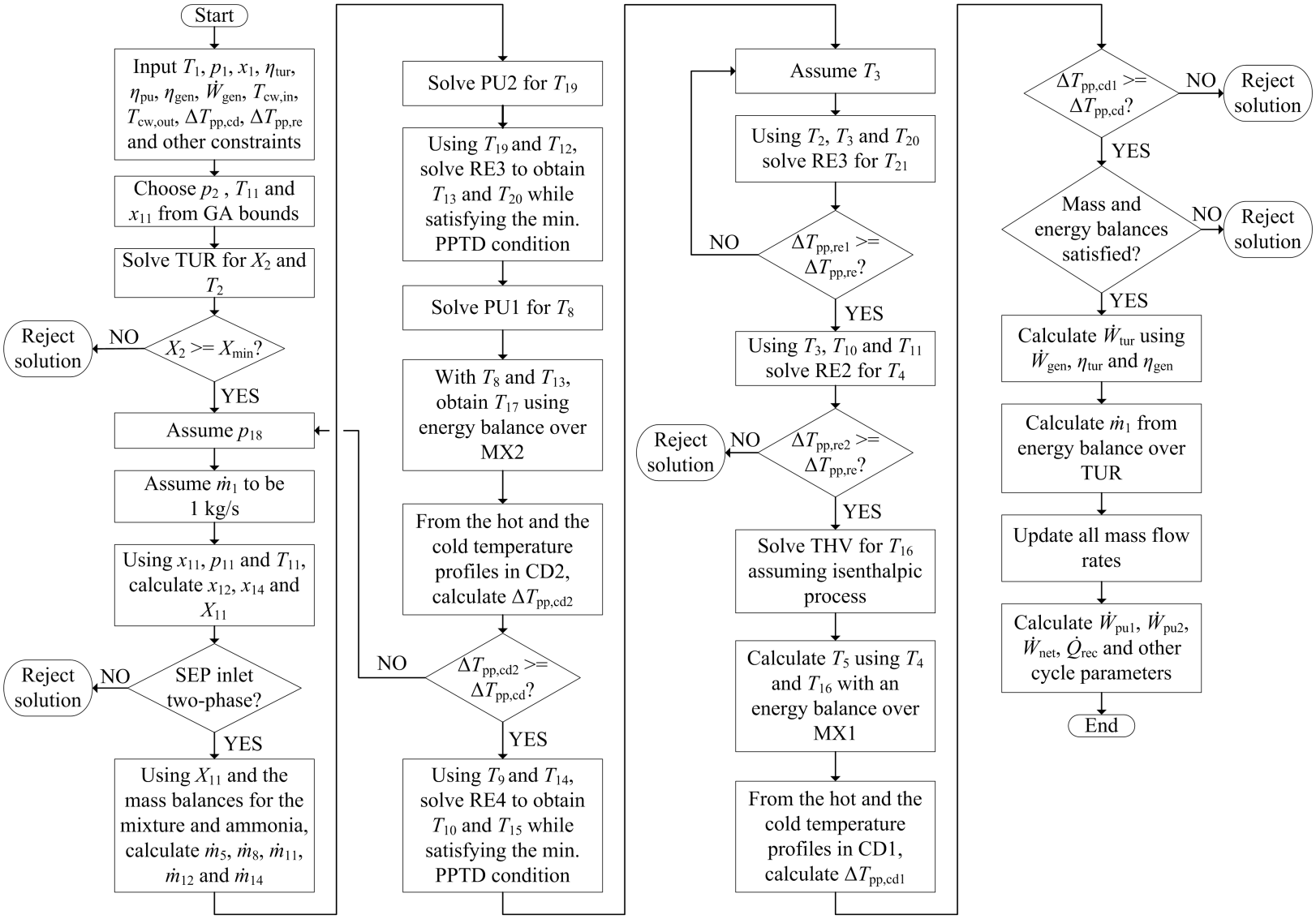


Figure 3: Solution algorithm for every iteration of the KC1234 layout.

The following assumptions were made for the cycle optimisation:

(a). The cycles were modelled in steady state.

(b). The turbine inlet temperature was fixed at 500 °C. The isentropic efficiency for the turbine was 85 % and for the pumps was 70 %. The turbine mechanical efficiency and the generator efficiency were both 98 %. The plant was designed for a generator output of 20 MW. The minimum allowed vapour quality at the turbine outlet was 90 %. The condenser cooling water inlet and outlet temperatures were fixed at 20 °C and 30 °C respectively.

(c). The minimum PPTD for the recuperators was 8 °C ($\Delta T_{\mathrm{pp,re}}$) and for the condensers was 4 °C ($\Delta T_{\mathrm{pp,cd}}$).

(d). A pressure drop of 8 % [21] was considered for the direct steam generation receiver. Pressure drops and heat losses in the other components of both the cycles were neglected.

(e). The minimum separator inlet vapour quality was fixed at 5 %.

## 3. Results

The optimal solutions for the four Kalina cycle layouts at different values of turbine inlet pressures and ammonia mass fractions are shown in Fig. 4.

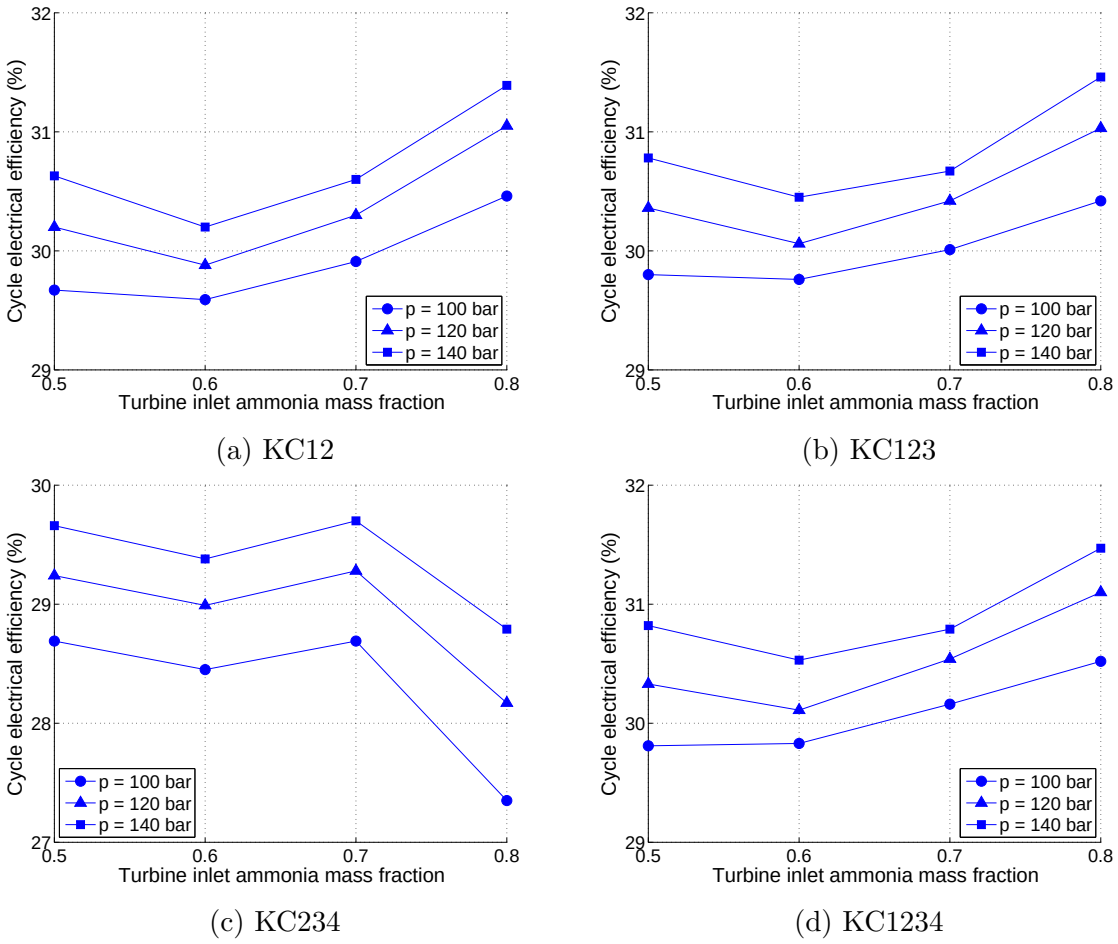


(a) KC12 (b) KC123

(c) KC234 (d) KC1234

Figure 4: Cycle efficiency at different turbine inlet pressures and ammonia mass fractions for the four Kalina cycle layouts.

It may be observed that except for the cycle efficiency curve for the KC234 layout (Fig. 4c), all other curves show similar trends. Obtaining an optimum value of the turbine inlet ammonia mass fraction around 0.7 for the KC234 layout is comparable to a similar trend observed in previous studies by Marston [10] and Nag and Gupta [13]. The cycle efficiency values are however different since the calculations of the thermodynamic properties were made with different methodologies and there were slightly different assumptions made in solving the cycle. This trend also demonstrates the effect of the number and placement of the different recuperators in the Kalina cycle. Combined with the previous observation by Modi and Haglind [15] for the KC12 layout that the highest cycle efficiency occurs near a

turbine inlet ammonia mass fraction of 0.9, since using pure ammonia significantly reduces the cycle efficiency, it seems that the optimum of the turbine inlet ammonia mass fraction could occur in very different range of values depending on the cycle layout.

Of all the compared configurations, the maximum cycle efficiency was obtained by the KC1234 layout, equal to 31.47 %, at a turbine inlet pressure and ammonia mass fraction of 140 bar and 0.8. The KC123 layout was a close second with a cycle efficiency of 31.46 % at a turbine inlet pressure and ammonia mass fraction of 140 bar and 0.8. The lowest cycle efficiency was obtained by the KC234 layout, equal to 27.35 %, at a turbine inlet pressure and ammonia mass fraction of 100 bar and 0.8. The maximum turbine inlet pressure was restricted at 140 bar so as to avoid supercritical operation with higher values of the turbine inlet ammonia mass fractions which would result in using complicated designs and more expensive, high pressure resistant materials.

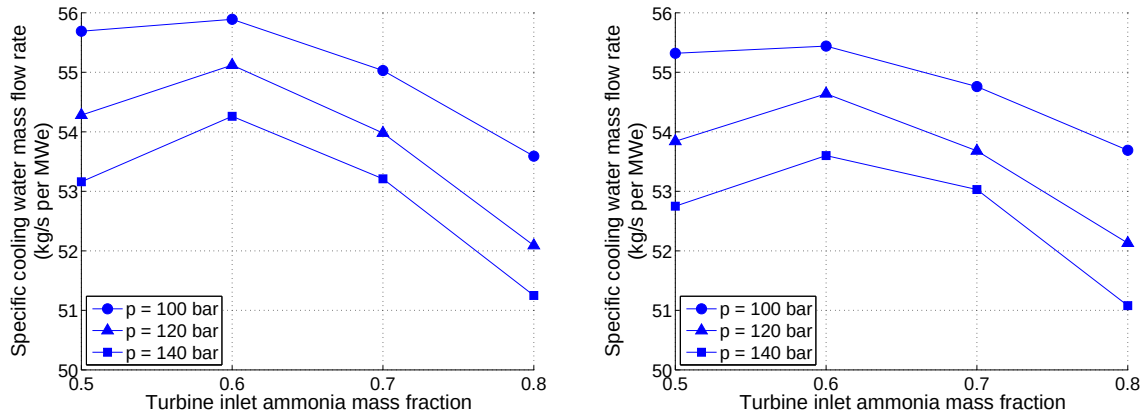


(a) KC12




(b) KC123

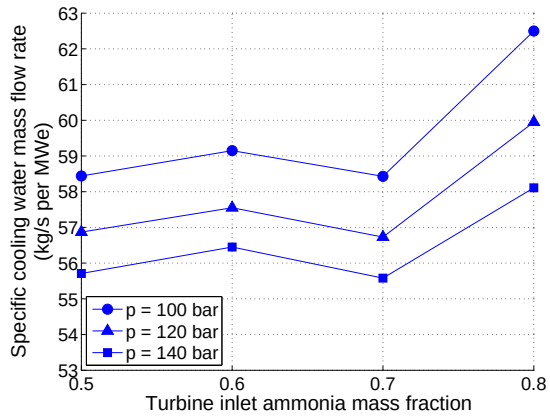


(c) KC234

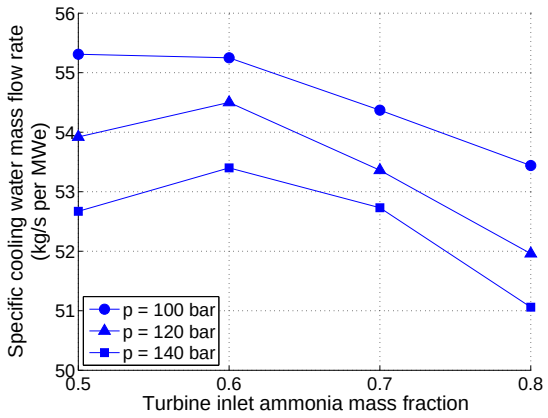


(d) KC1234

Figure 5: Cooling water mass flow rate per MW of net electrical power output for the four Kalina cycle layouts at different turbine inlet pressures and ammonia mass fractions (combined for both the condensers).

The condenser cooling water requirement for the four Kalina cycle layouts at different turbine inlet pressures and ammonia mass fractions is shown in Fig. 5. The cooling water mass flow rates are per MW of the net electrical power output to have a fair comparison. The water requirement for both the condensers (CD1 and CD2) was added to get the total water requirement for the cycle. It may be observed that the condenser cooling water flow rates exhibit a trend related to the respective cycle efficiency figures, i.e., the better the cycle efficiency, the less is the cooling water requirement. This behaviour is expected as the more effective is the condensation process, the lower is the cooling load resulting in better cycle efficiency values.

## 4. Discussion

A Kalina cycle layout suitable for high temperature applications is inherently complex in nature with the presence of several recuperators, condensers, pumps and an internal separator loop. Solving such a cycle with high computational efficiency presents a significant challenge. Several authors have made different assumptions previously in order to approach this problem from different angles. However, some of those assumptions are inappropriate given the zeotropic nature of the ammonia-water mixture. Marston [10] presented a methodology to solve such a Kalina cycle by assuming the separator inlet ammonia mass fraction for a specified separator inlet temperature to begin the iteration. He proposed to calculate the mass flow rates using a simplified layout of the cycle and then solve the internal loop in the cycle using mass and energy balances until the separator inlet ammonia mass fraction calculated at the end is within acceptable tolerance of the initially guessed value. During this process, he also assumed that the pinch point in the condensers would always occur at the cooling water inlet point of the condenser. This is not valid for ammonia-water mixtures with high ammonia mass fractions and may lead to incorrect condenser pressure calculations. Nag and Gupta [13] used a similar approach, however they did not explain it in detail in their paper.

In the current study, instead of solving the cycle by assuming an initial guess value for the separator inlet ammonia mass fraction, this parameter is considered as a decision variable for the GA. This reduced the computational time significantly, especially when running the simulations with higher values of turbine inlet ammonia mass fractions. As an example, for KC234, a layout similar to the one presented by Marston [10], the cycle optimisation with a turbine inlet pressure of 100 bar and a turbine inlet ammonia mass fraction of 0.5 was completed in about 50 min using the latter approach compared with about 11 h using the approach as explained by Marston [10]. This is primarily because it is much faster to calculate the thermodynamic properties using the ammonia mass fraction as an input rather than trying to iteratively solve for the ammonia mass fraction in a close range of temperature values.

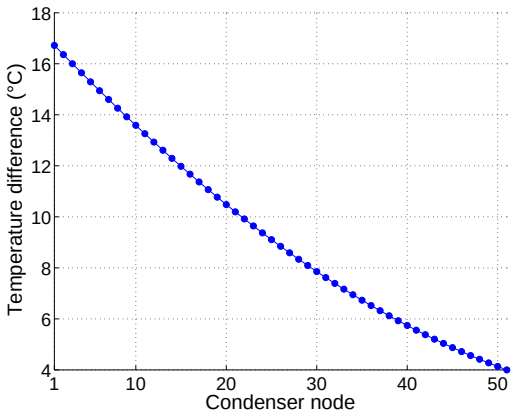


(a) 0.5 working fluid ammonia mass fraction

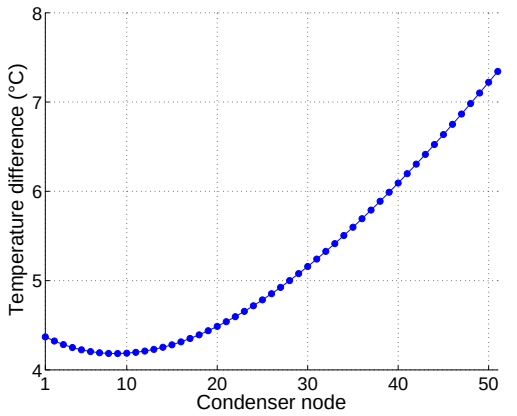


(b) 0.8 working fluid ammonia mass fraction

Figure 6: Temperature difference between the hot and the cold fluids over the condenser-2 for KC1234 for different working fluid compositions at a turbine inlet pressure of 100 bar.

The temperature difference between the working fluid and the condenser cooling water over the condenser-2 for the KC1234 layout is shown in Fig. 6a. The curve is for the optimum solution at a turbine inlet pressure of 100 bar and the working fluid ammonia mass fraction of 0.5. The condenser was divided into 50 control volumes to evaluate the pinch point, thus resulting in 51 nodes as the nodes were assumed at the boundaries of the control volumes. The node 1 in the curve is where the cooling water *exits* the condenser, i.e., the node where the working fluid enters the condenser, given the assumption of counter-flow heat exchanger. Fig. 6b shows the same curve, but for a working fluid ammonia mass fraction of 0.8. These figures clearly show that the PPTD (the lowest point in the curve, close to 4 °C) occurs at very different positions in the condenser when the working fluid ammonia mass fraction is changed. This is primarily due to the change in the convexity of the temperature profile of the ammonia-water mixtures with changing ammonia mass fraction, as also elaborated by Kim et al. [22]. Therefore, an assumption of a fixed position for the pinch point will not only result in a calculation of an incorrect condenser pressure, but possibly also in a violation of the second law of thermodynamics. The assumption of a constant overall LMTD for the heat exchangers might also produce similar results, or unusually low PPTDs.

It is also possible to use the turbine inlet pressure and ammonia mass fractions as additional decision variables for the optimisation, but at the cost of computational time. It was not done in this study since the purpose here is to demonstrate the trend of the cycle performance parameters and provide an efficient optimisation and solution algorithm, rather than finding the optimum values of turbine inlet pressure and ammonia mass fraction.

An overview of the heat transfer in the key components of the cycle, i.e., the heat recuperation within the cycle, the heat rejected by the cycle during condensation (cooling load) and the heat input to the receiver (heating load), is provided in the Table 2. The presented values are for that combination of the turbine inlet pressure and ammonia mass fraction for the four layouts which resulted in the highest cycle efficiency among the compared cases.

Table 2: Heat transfer in the key components for the four layouts at a turbine inlet pressure of 140 bar.

| | KC12 ($x$=0.8) | KC123 ($x$=0.8) | KC234 ($x$=0.7) | KC1234 ($x$=0.8) |
|---|---|---|---|---|
| $\dot{Q}_{re1}$ [MW] | 15.57 | 14.92 | - | 14.06 |
| $\dot{Q}_{re2}$ [MW] | 18.56 | 19.10 | 26.09 | 17.64 |
| $\dot{Q}_{re3}$ [MW] | - | 0.58 | 7.42 | 1.38 |
| $\dot{Q}_{re4}$ [MW] | - | - | 7.83 | 2.55 |
| $\dot{Q}_{cd1}$ [MW] | 26.70 | 26.92 | 30.42 | 26.89 |
| $\dot{Q}_{cd2}$ [MW] | 14.27 | 13.90 | 14.31 | 13.93 |
| $\dot{Q}_{rec}$ [MW] | 60.91 | 60.76 | 64.79 | 60.77 |

The results from the KC12, the KC123 and the KC1234 layouts exhibit similar trends for the cycle efficiency (Figs. 4a, 4b and 4d, respectively). This trend of the variation in the cycle efficiency with the turbine inlet pressure and ammonia mass fraction was explained in detail for the KC12 layout by Modi and Haglind [15]. In short, the rate of exergy destruction in the two condensers, the recuperator-1 and the turbine shows a decreasing trend; whereas the rate of exergy destruction in the recuperator-2 first increases and then decreases. Similarly, the

rate of exergy destruction in the throttle valve and the mixers becomes negligible at higher values of turbine inlet ammonia mass fraction due to a better match between the mixing streams' temperatures. The combination of these trends causes the cycle efficiency to first drop and then increase after reaching a minimum value. A similar explanation is also valid for the KC123 and the KC1234 layouts as most of the heat recovery is still in the recuperators 1 and 2, and there is small additional heat recovery in the recuperators 3 and 4. The KC234 layout, on the other hand, presents an optimum value of the turbine inlet ammonia mass fraction around 0.7 for maximum cycle efficiency. The reason for having a different trend in the KC234 layout can be attributed to the absence of the recuperator-1 which is a common feature in the other three layouts. Moreover, as may be observed from Table 2, the cooling load in the KC234 layout is the maximum, thus resulting in a larger loss of energy in the condensers as compared with the other three layouts. This also significantly affects the cycle efficiency in a negative manner. An overview of the typical operation condition for the four layouts is presented in the Appendix A for the best performing configurations among the considered cases.

The analysis presented in this paper considered a central receiver solar thermal power plant with direct steam generation as a case study for high temperature and pressure Kalina cycle applications. The cycles were optimised for a fixed generator power rating. However, this approach can be also be used for other applications such as a bottoming cycle for a gas turbine, waste heat recovery, geothermal power plants and other types of concentrating solar power plants with slight modifications. These modifications would be the addition of a few heat exchangers which will transfer the heat from a hot fluid to the Kalina cycle working fluid and additional pinch point evaluations for these heat exchangers. In case the heat input is a fixed quantity as in a waste heat recovery plant, the energy available in the hot fluid stream shall be an input to the optimiser (by mentioning the inlet and the outlet temperatures and the mass flow rate), instead of the design generator rating. The objective function in such cases shall be to maximise the specific power output from the plant. It is also possible to covert the objective function to a thermoeconomic one, while using a similar approach to solve the cycle, by maximising the net present value or minimising the

levelized cost of electricity. This could be done by simply adding the relevant heat transfer correlations for the calculation of the heat exchanger areas, and the cost functions for the different cycle components.

## 5. Conclusion

Four Kalina cycle layouts for high temperature and pressure applications were optimised and compared based on different performance parameters such as the cycle efficiency and the cooling water requirement. A detailed methodology for solving and optimising these layouts is presented with a central receiver solar thermal power plant with direct steam generation as the considered case. It is observed that the placement and the number of the recuperators in the cycle plays an important role in determining the cycle performance. This might result in obtaining a very different optimum value of the turbine inlet ammonia mass fraction for maximum cycle efficiency. Among the compared layouts, the KC1234 layout gives the highest cycle efficiency of 31.47 % at a turbine inlet pressure and ammonia mass fraction of 140 bar and 0.8, but the layout KC123 was close second with a cycle efficiency of 31.46 % at a turbine inlet pressure and ammonia mass fraction of 140 bar and 0.8. The lowest cycle efficiency was obtained by the KC234 layout, equal to 27.35 %, at a turbine inlet pressure and ammonia mass fraction of 100 bar and 0.8.

The presented optimisation algorithm is based on improved assumptions as compared with the previous studies and is computationally efficient. The optimisation objective was maximisation of the cycle electrical efficiency while using the turbine outlet pressure, the separator inlet temperature and the separator inlet ammonia mass fraction as the decision variables. This approach can also be used for other Kalina cycle applications such as a bottoming cycle, for waste heat recovery, geothermal power plants and other types of concentrating solar power plants with minor modifications specific to the case at hand.

## Appendix A. Typical operation state points

Tables A.1 to A.4 show the operating conditions of the most efficient configuration among the considered cases for the four Kalina cycle layouts. In the tables, $T$ is the mixture

temperature, $p$ is the pressure, $\dot{m}$ is the mass flow rate, $x$ is the ammonia mass fraction and $h$ is the specific enthalpy.

Table A.1: Operation state points for KC12 at turbine inlet pressure and ammonia mass fraction of 140 bar and 0.8.

| Stream | $T$ (°C) | $p$ (bar) | $\dot{m}$ (kg/s) | $x$ | $h$ (kJ/kg) |
|---|---|---|---|---|---|
| 1 | 500.0 | 140.00 | 29.27 | 0.8000 | 2902.4 |
| 2 | 183.9 | 6.04 | 29.27 | 0.8000 | 2190.9 |
| 3 | 93.0 | 6.04 | 29.27 | 0.8000 | 1658.8 |
| 4 | 38.6 | 6.04 | 29.27 | 0.8000 | 1024.7 |
| 5 | 43.4 | 6.04 | 47.15 | 0.6795 | 699.0 |
| 6 | 24.0 | 6.04 | 47.15 | 0.6795 | 132.7 |
| 7 | 24.1 | 8.20 | 47.15 | 0.6795 | 133.1 |
| 8 | 24.1 | 8.20 | 18.00 | 0.6795 | 133.1 |
| 9 | 24.1 | 8.20 | 29.15 | 0.6795 | 133.1 |
| 10 | 56.0 | 8.20 | 29.15 | 0.6795 | 769.9 |
| 11 | 56.0 | 8.20 | 11.27 | 0.9925 | 1728.4 |
| 12 | 56.0 | 8.20 | 17.88 | 0.4823 | 166.0 |
| 13 | 47.8 | 6.04 | 17.88 | 0.4823 | 166.0 |
| 14 | 34.3 | 8.20 | 29.27 | 0.8000 | 747.2 |
| 15 | 27.0 | 8.20 | 29.27 | 0.8000 | 259.8 |
| 16 | 31.0 | 152.17 | 29.27 | 0.8000 | 289.3 |
| 17 | 134.2 | 152.17 | 29.27 | 0.8000 | 821.3 |

## References


[1] A.I. Kalina. Combined-cycle system with novel bottoming cycle. *Journal of Engineering for Gas Turbines and Power*, 106:737–742, 1984.

[2] S. Ogriseck. Integration of Kalina cycle in a combined heat and power plant, a case study. *Applied Thermal Engineering*, 29(14-15):2843–2848, 2009.

[3] P. Bombarda, C.M. Invernizzi, and C. Pietra. Heat recovery from diesel engines: A thermodynamic comparison between Kalina and ORC cycles. *Applied Thermal Engineering*, 30(2-3):212–219, 2010.

[4] O.K. Singh and S.C. Kaushik. Energy and exergy analysis and optimization of Kalina cycle coupled with a coal fired steam power plant. *Applied Thermal Engineering*, 51(1-2):787–800, 2013.

[5] A. Coskun, A. Bolatturk, and M. Kanoglu. Thermodynamic and economic analysis and optimization of power cycles for a medium temperature geothermal resource. *Energy Conversion and Management*, 78:39–49, February 2014.

[6] J. Wang, Z. Yan, E. Zhou, and Y. Dai. Parametric analysis and optimization of a Kalina cycle driven by solar energy. *Applied Thermal Engineering*, 50(1):408–415, 2013.

[7] F. Sun, W. Zhou, Y. Ikegami, K. Nakagami, and X. Su. Energy-exergy analysis and optimization of the solar-boosted Kalina cycle system 11 (KCS-11). *Renewable Energy*, 66:268–279, 2014.

[8] U. Larsen, L. Pierobon, J. Wronski, and F. Haglind. Multiple regression models for the prediction of the maximum obtainable thermal efficiency of organic Rankine cycles. *Energy*, 65:503–510, 2014.

[9] T.-V. Nguyen, T. Knudsen, U. Larsen, and F. Haglind. Thermodynamic evaluation of the Kalina split-cycle concepts for waste heat recovery applications. *Energy*, 71:277–288, 2014.

[10] C.H. Marston. Parametric analysis of the Kalina cycle. *Journal of Engineering for Gas Turbines and Power*, 112:107–116, 1990.

[11] C.H. Marston and M. Hyre. Gas turbine bottoming cycles: Triple-pressure steam versus Kalina. *Journal of Engineering for Gas Turbines and Power*, 117(January):10–15, 1995.

[12] M.B. Ibrahim and R.M. Kovach. A Kalina cycle application for power generation. *Energy*, 18(9):961–969, 1993.

[13] P.K. Nag and A.V.S.S.K.S. Gupta. Exergy analysis of the Kalina cycle. *Applied Thermal Engineering*, 18(6):427–439, 1998.

[14] E. Thorin. *Power cycles with ammonia-water mixtures as working fluid.* Phd thesis, KTH Royal Institute of Technology, Stockholm, Sweden, 2000.

[15] A. Modi and F. Haglind. Performance analysis of a Kalina cycle for a central receiver solar thermal power plant with direct steam generation. *Applied Thermal Engineering*, 65(1-2):201–208, 2014.

[16] X. Zhang, M. He, and Y. Zhang. A review of research on the Kalina cycle. *Renewable and Sustainable Energy Reviews*, 16(7):5309–5318, 2012.

[17] MathWorks. MATLAB. www.mathworks.se/products/matlab/, 2014. Accessed 22/06/2014.

[18] National Institute for Standards and Technology. REFPROP MATLAB Interface. www.boulder.nist.gov/div838/theory/refprop/Frequently_asked_questions.htm# MatLabApplications, 2013. Accessed 30/08/2014.

[19] R. Tillner-Roth and D.G. Friend. A Helmholtz free energy formulation of the thermodynamic properties

of the mixture {water+ammonia}. *Journal of Physical and Chemical Reference Data*, 27(1):63–96, 1998.

[20] E. Lemmon. Personal communication, 2013.

[21] B. Koretz, L. Afremov, O. Chernin, and C. Rosin. Molten salt thermal energy storage for direct steam tower systems. In *Proceedings of SolarPACES Concentrating Solar Power and Chemical Energy Systems*, Granada, Spain, 2011.

[22] K.H. Kim, C.H. Han, and K. Kim. Effects of ammonia concentration on the thermodynamic performances of ammoniawater based power cycles. *Thermochimica Acta*, 530:7–16, 2012.

Table A.2: Operation state points for KC123 at turbine inlet pressure and ammonia mass fraction of 140 bar and 0.8.

| Stream | $T$ (°C) | $p$ (bar) | $\dot{m}$ (kg/s) | $x$ | $h$ (kJ/kg) |
|---|---|---|---|---|---|
| 1 | 500.0 | 140.00 | 29.20 | 0.8000 | 2902.4 |
| 2 | 183.2 | 5.98 | 29.20 | 0.8000 | 2189.3 |
| 3 | 93.9 | 5.98 | 29.20 | 0.8000 | 1678.4 |
| 4 | 38.4 | 5.98 | 29.20 | 0.8000 | 1024.5 |
| 5 | 41.2 | 5.98 | 52.26 | 0.6723 | 642.9 |
| 6 | 24.2 | 5.98 | 52.26 | 0.6723 | 127.7 |
| 7 | 24.3 | 8.28 | 52.26 | 0.6723 | 128.1 |
| 8 | 24.3 | 8.28 | 17.63 | 0.6723 | 128.1 |
| 9 | 24.3 | 8.28 | 34.62 | 0.6723 | 128.1 |
| 10 | 52.0 | 8.28 | 34.62 | 0.6723 | 679.7 |
| 11 | 52.0 | 8.28 | 11.57 | 0.9946 | 1716.3 |
| 12 | 39.3 | 8.28 | 11.57 | 0.9946 | 1666.0 |
| 13 | 52.0 | 8.28 | 23.05 | 0.5106 | 159.4 |
| 14 | 43.1 | 5.98 | 23.05 | 0.5106 | 159.4 |
| 15 | 34.3 | 8.28 | 29.20 | 0.8000 | 737.4 |
| 16 | 27.3 | 8.28 | 29.20 | 0.8000 | 261.4 |
| 17 | 31.3 | 152.17 | 29.20 | 0.8000 | 290.9 |
| 18 | 35.3 | 152.17 | 29.20 | 0.8000 | 310.8 |
| 19 | 134.3 | 152.17 | 29.20 | 0.8000 | 821.7 |

Table A.3: Operation state points for KC234 at turbine inlet pressure and ammonia mass fraction of 140 bar and 0.7.

| Stream | $T$ (°C) | $p$ (bar) | $\dot{m}$ (kg/s) | $x$ | $h$ (kJ/kg) |
|---|---|---|---|---|---|
| 1 | 500.0 | 140.00 | 26.09 | 0.7000 | 2948.4 |
| 2 | 127.9 | 3.05 | 26.09 | 0.7000 | 2150.3 |
| 3 | 59.9 | 3.05 | 26.09 | 0.7000 | 1150.2 |
| 4 | 58.5 | 3.05 | 52.95 | 0.4782 | 578.8 |
| 5 | 24.6 | 3.05 | 52.95 | 0.4782 | 4.3 |
| 6 | 24.6 | 6.40 | 52.95 | 0.4782 | 4.9 |
| 7 | 24.6 | 6.40 | 12.54 | 0.4782 | 4.9 |
| 8 | 24.6 | 6.40 | 40.41 | 0.4782 | 4.9 |
| 9 | 51.5 | 6.40 | 40.41 | 0.4782 | 198.6 |
| 10 | 93.0 | 6.40 | 40.41 | 0.4782 | 844.2 |
| 11 | 93.0 | 6.40 | 13.55 | 0.9051 | 1892.4 |
| 12 | 35.8 | 6.40 | 13.55 | 0.9051 | 1344.9 |
| 13 | 93.0 | 6.40 | 26.86 | 0.2628 | 315.3 |
| 14 | 32.6 | 6.40 | 26.86 | 0.2628 | 23.8 |
| 15 | 32.7 | 3.05 | 26.86 | 0.2628 | 23.8 |
| 16 | 41.0 | 6.40 | 26.09 | 0.7000 | 701.1 |
| 17 | 24.5 | 6.40 | 26.09 | 0.7000 | 152.8 |
| 18 | 27.8 | 152.17 | 26.09 | 0.7000 | 180.6 |
| 19 | 84.0 | 152.17 | 26.09 | 0.7000 | 465.0 |

Table A.4: Operation state points for KC1234 at turbine inlet pressure and ammonia mass fraction of 140 bar and 0.8.

| Stream | $T$ (°C) | $p$ (bar) | $\dot{m}$ (kg/s) | $x$ | $h$ (kJ/kg) |
|---|---|---|---|---|---|
| 1 | 500.0 | 140.00 | 29.18 | 0.8000 | 2902.4 |
| 2 | 182.9 | 5.96 | 29.18 | 0.8000 | 2188.7 |
| 3 | 95.3 | 5.96 | 29.18 | 0.8000 | 1706.8 |
| 4 | 44.8 | 5.96 | 29.18 | 0.8000 | 1102.3 |
| 5 | 46.1 | 5.96 | 45.08 | 0.6726 | 723.7 |
| 6 | 24.1 | 5.96 | 45.08 | 0.6726 | 127.2 |
| 7 | 24.1 | 8.28 | 45.08 | 0.6726 | 127.7 |
| 8 | 24.1 | 8.28 | 17.36 | 0.6726 | 127.7 |
| 9 | 24.1 | 8.28 | 27.73 | 0.6726 | 127.7 |
| 10 | 35.7 | 8.28 | 27.73 | 0.6726 | 219.5 |
| 11 | 64.0 | 8.28 | 27.73 | 0.6726 | 855.8 |
| 12 | 64.0 | 8.28 | 11.83 | 0.9870 | 1752.1 |
| 13 | 39.3 | 8.28 | 11.83 | 0.9870 | 1635.5 |
| 14 | 64.0 | 8.28 | 15.90 | 0.4388 | 189.2 |
| 15 | 32.1 | 8.28 | 15.90 | 0.4388 | 29.0 |
| 16 | 32.2 | 5.96 | 15.90 | 0.4388 | 29.0 |
| 17 | 34.3 | 8.28 | 29.18 | 0.8000 | 738.7 |
| 18 | 27.3 | 8.28 | 29.18 | 0.8000 | 261.4 |
| 19 | 31.3 | 152.17 | 29.18 | 0.8000 | 290.9 |
| 20 | 40.8 | 152.17 | 29.18 | 0.8000 | 338.1 |
| 21 | 134.0 | 152.17 | 29.18 | 0.8000 | 820.1 |